JOURNAL OF MATERIALS SCIENCE **39** (2004) 3635–3639

Capacity fading of $LiMn_2O_4$ electrode: Influence of calcination temperature

J. T. SON*, K. S. PARK, H. G. KIM
Department of Materials Science and Engineering, Korea Advanced Institute of Science and Technology, 373-1 Kusong-dong, Yusong-gu, Taejon, Korea
E-mail: sonjongtae@kaist.ac.kr

H. T. CHUNG
Department of Ceramic Engineering, Dong-shin University, 252 Naju, Chonnam 520-714, Korea

Spinel-type Li-Mn oxides of formula $LiMn_{2-x}O_4$ were prepared by the Pechini method in the range of 600–850°C for 4 h. These spinels were investigated by X-ray powder diffraction, SEM (scanning electron microscope), ICP, chemical titration and galvanostatic cycling at 0.2C rates. The effect of calcination temperature is evaluated. With increasing calcination temperature, Mn valence-state of the powder decreased while size of powder increased. The cycle life of the powder decreases with increasing calcination temperature. The results indicated that the Mn valence-state and powder size of cathode powder should be important variables to improve cycle life. The effect of cell polarization effect on the cycle life is also discussed. © *2004 Kluwer Academic Publishers*

1. Introduction

Layered $LiCoO_2$, $LiNiO_2$ and spinel $LiMn_2O_4$ could be used as the cathode materials of the lithium battery [1–5] because of their high voltage (about 4 V) and good rechargeability. Among these materials, $LiMn_2O_4$ is the most favored because of its low cost and environmental friendly character [6–8]. For the past ten years, the spinel $LiMn_2O_4$ has been studied extensively as a positive electrode material for rechargeable lithium and lithium ion cells [6–8]. However, the $LiMn_2O_4$ electrodes have showed capacity fading during cycling [6–8]. Several possible reasons about capacity fading are suggested; such as an organic-based electrolyte in a high potential region [2], the dissolution of manganese into electrolyte [3], Jahn-Teller distortion due to Mn^{3+} ion [2], change in crystal uniformity with cycling [4], and so on.

In this work, we measured Mn valence-state of $LiMn_2O_4$ as a function of calcination temperature by using ICP and chemical titration method and mean powder size by using powder size analyzer. Taking advantage of these analysis methods, we can speculate the origin of capacity fading mechanism. This paper aims to elucidate the effect of calcination temperature on the composition, the microstructure and the electrochemical properties of $LiMn_2O_4$ electrodes.

2. Experimental

2.1. Powder preparation

In the present study, we have adapted the modified Pechini process [9–11] to the synthesis of $LiMn_2O_4$. The process is based on the ability of certain weak acids to form polybasic acid chelates with various cations [9]. These chelates can undergo poly-esterification when heated in a polyhydroxyl alcohol to form a solid polymeric resin throughout which the cations are uniformly distributed [9]. Thus the resin retains homogeneity on the atomic scale and may be calcined at low temperature to yield fine oxides. Using this method, it is possible to obtain phase-pure ultrafine crystalline spinel phases after firing the polymeric precursors at low temperatures. The Pechini process was originally developed to prepare metal oxide powders such as titanates and niobates for capacitor [9]. Reagents of $MnCO_3$ (Junsei Chemicals; 99%), $LiNO_3$ (Junsei Chemicals; 99%), CA (citric acid: Aldrich Chemicals; 99.5%), EG (ethylene glycol: Acros Organics; 99%) were used as starting materials. $MnCO_3$ was dissolved in dilute nitric acid with several drops of hydrogen peroxide (Junsei Chemicals; 30%) until a clear solution was obtained.

Pre-dissolved solutions of CA and EG with a molar ratio ($R = 2$) of EG to CA was added to the clear cation solutions. The mixed solutions were stirred on a hot plate, which allowed the temperature to be controlled

---

*Author to whom all correspondence should be addressed.

0022–2461 © *2004 Kluwer Academic Publishers*

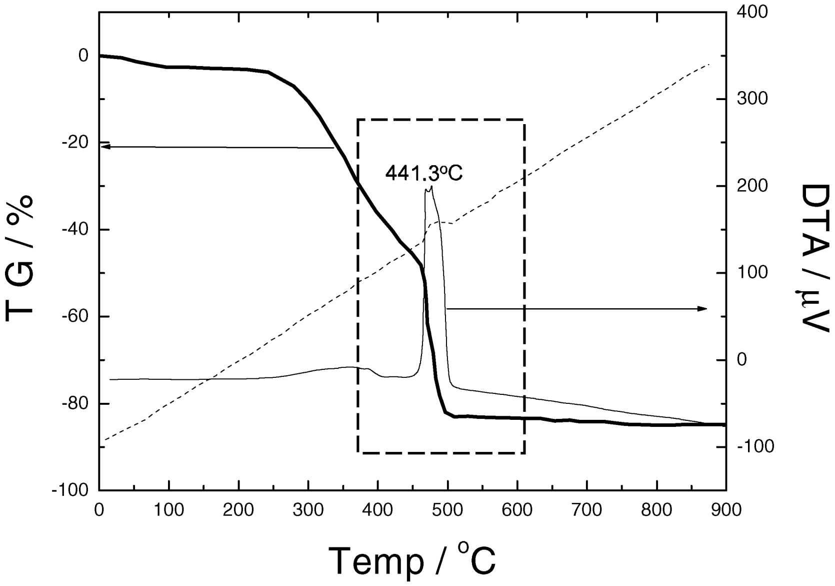

Figure 1 TG-DTA curve for $LiMn_2O_4$ precursor powder after air drying at 150°C for 24 h: ramp rate of 5°C/min.

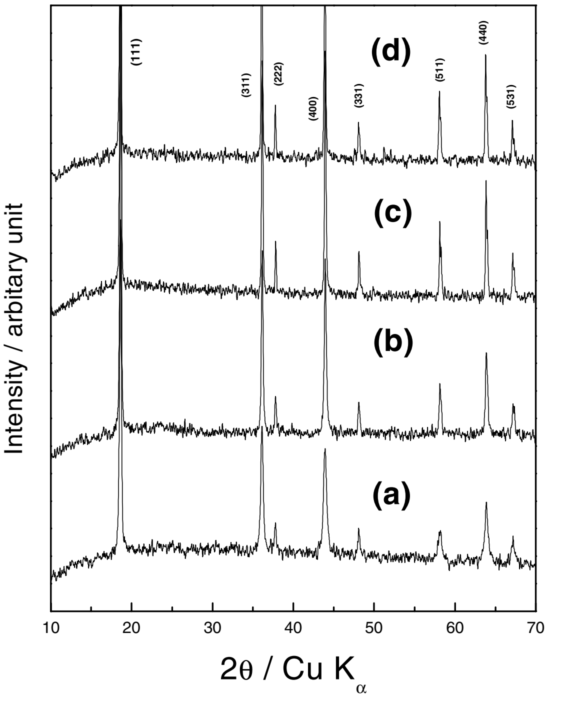

Figure 2 X-ray diffraction patterns of $LiMn_2O_4$ powder calcined at: (a) 600°C for 4 h, (b) 700°C for 4 h, (c) 800°C for 4 h and (d) 850°C for 4 h.

below 200°C, until the solutions become a dark-brown gel. Drying in oven to evaporate the residual water at 150°C were followed and a puffed char was obtained. The puffed precursors were self-ignited by increasing oven temperature at 250°C in air. The ignited powders were calcined in a furnace at 600–850°C for 4 h in air.

The thermal decomposition behavior of the dried precursors was examined by using thermo-gravimetry (TG) and differential scanning calorimeter (DSC) at a heating rate of 5°C/min with a STA409 instrument. Phase analysis was carried out by powder X-ray diffraction (XRD) with Cu K_α radiation in a Rigaku X-ray diffractometer. Scanning electron microscopes

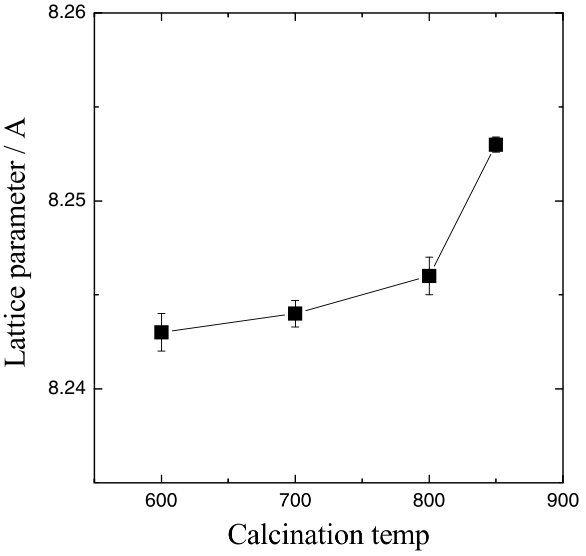

Figure 3 Variation of lattice parameter of $LiMn_2O_4$ powder calcined at: (a) 600°C, (b) 700°C for 4 h, (c) 800°C for 4 h and (d) 850°C for 4 h.

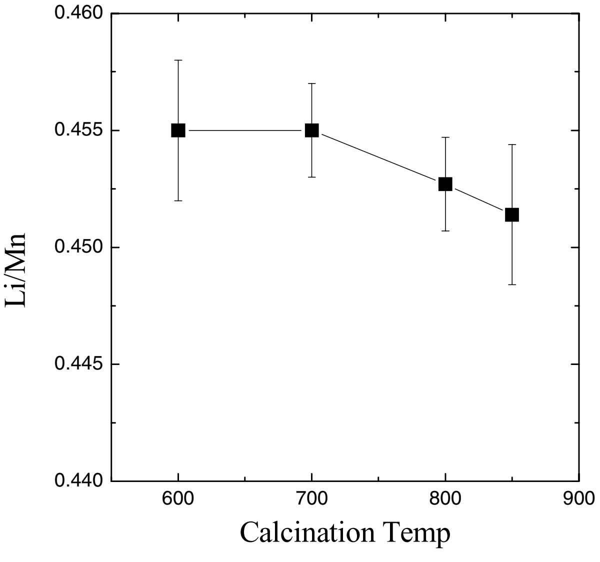

Figure 4 Relative Li/Mn contents of $LiMn_2O_4$ powder according to calcination temperature.

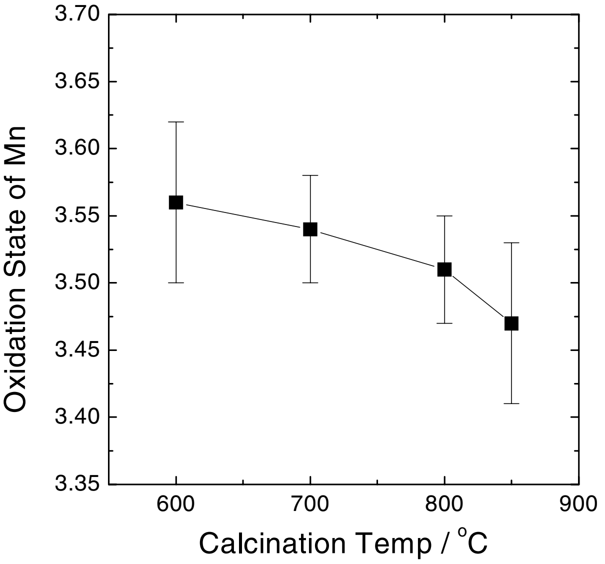

Figure 5 Mn valence state of $LiMn_2O_4$ powder calcined at different temperatures for 4 h.

(SEM) were obtained to examine the morphology of the powder.

The chemical composition of these samples was analyzed by using an inductively coupled plasma atomic emission spectroscopy (ICP-AES). The average oxidation state of manganese was determined by titration with $KMnO_4$. About 0.3 g of the sample was dissolved in 20 ml of $VOSO_4$ solution. During dissolution higher Mn oxidation of (III) and (IV) are reduced Mn(II) by the oxidation states of V(IV) to V(V). The excess V(IV) is back titrated with 0.1 M $KMnO_4$. Having titrated the excess V(IV) all of the manganese is present as Mn(II), and this amount is determined by further titration with by $KMnO_4$ in the presence of a complexing agent in which the manganese is oxidized to Mn(III). The titration reaction can be expressed as follows:

$$Mn^{(2+\eta)} + \eta V^{4+} \rightarrow \eta V^{5+} + Mn^{2+}$$

$$Mn^{(7+)} + 5V^{4+} \rightarrow 5V^{5+} + Mn^{2+}$$

From the titration, the oxidation of manganese can be calculated from charge neutrality assumption and Li/Mn ratio (analyzed by ICP-AES).

The average particle size of lithium manganese oxides was measured using particle size analyzer.

2.2. Electrochemical measurements

A cathode electrode was prepared by mixing $LiMn_2O_4$ powder with 10-wt% carbon black (Vulcan, XC-72) and 5-wt%PVDF (poly-vinylidene fluoride) in NMP (n-methyl pyrrodinone) solution. The stirred mixture was spread on a 316 stainless steel ex-met. The electrode specimens were dried under a vacuum at 120°C.

A three-electrode cell was constructed for charge-discharge experiments. Lithium foil (Foote Mineral, 99.9%) was used as the reference and counter-electrodes, and a 1 M $LiClO_4$-PC solution (pre-mixed at Mitsubishi Chemicals) was used as the electrolyte.

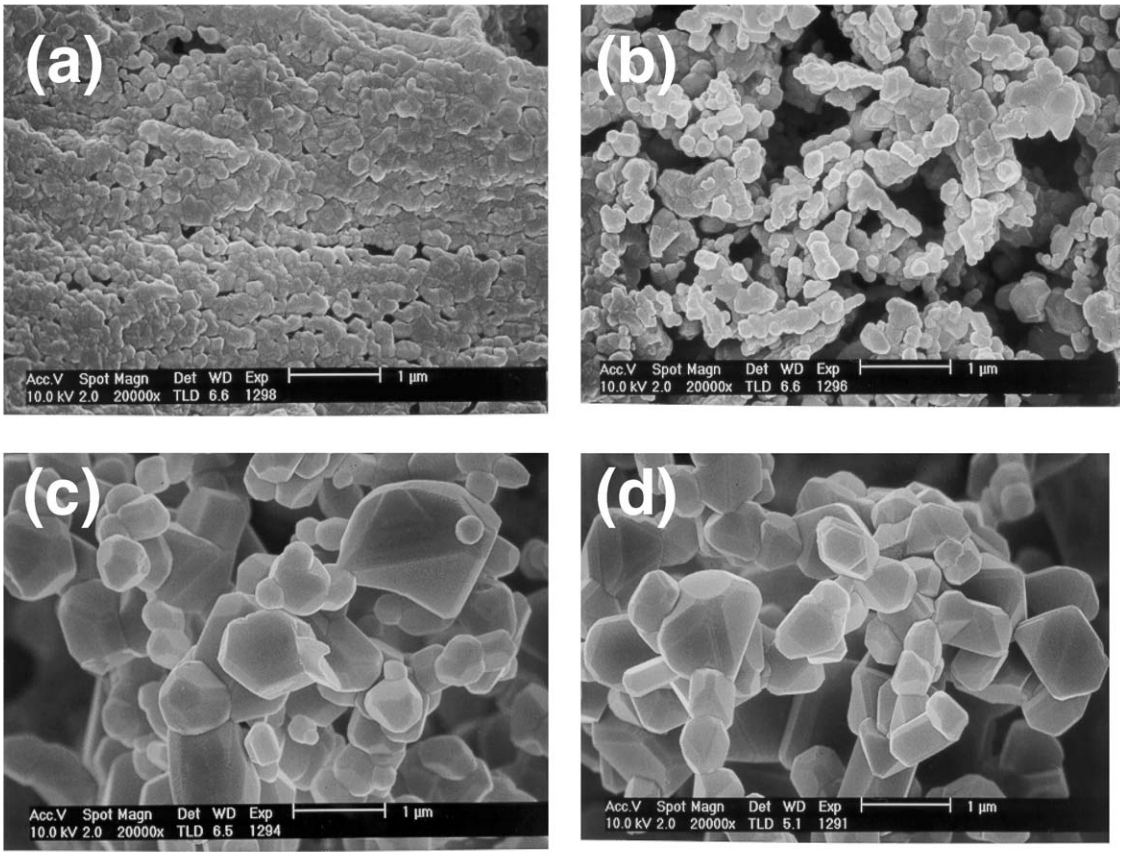

Figure 6 Electron microscopes of calcined at: (a) 600°C, (b) 700°C, (c) 800°C for 4 h, and (d) 850°C.

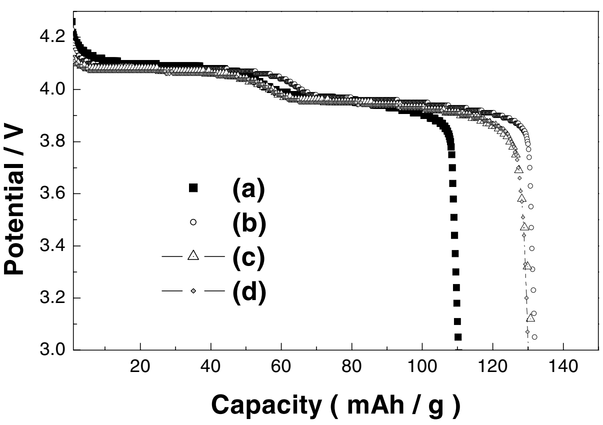

Figure 7 Initial discharge behavior of $LiMn_2O_4$: (a) 600°C for 4 h, (b) 700°C for 4 h, (c) 800°C for 4 h and (d) 850°C for 4 h.

Galvanostatic charge-discharge experiments were performed using a potentiostat/galvanostat (EG&G PARC Model 263). The cut-off voltages were set at 4.3 and 3.0 V for charge and discharge, respectively, at a current rate of 0.2 C.

3. Results and discussion

3.1. Powder preparation

The thermal decomposition behavior of precursor is presented in Fig. 1. The severe weight loss was observed from 250 to 500°C. There is a major exothermic peak near 440°C. It is concluded that most of the organic substances in the precursors are burned out at this temperature.

The XRD patterns of calcined powder are presented in Fig. 2. The calcined powders were indexed as pure single-phase spinel. The lattice parameter is plotted in Fig. 3 as a function of calcination temperature. The lattice parameter increases with increasing calcination temperature. Yoshio *et al.* [12] have reported that smaller cell volume usually shows good rechargeability. We can predict that the rechargeability will improve by using lithium-rich or low temperature calcination. The relative lithium contents using ICP are given in Fig. 4. In this figure, we can observe the evaporation of lithium above 800°C calcination. Fig. 5 shows that observed average oxidation state of manganese in the $Li_{1+x}Mn_{2-\delta}O_4$ by using chemical titration decreases with increasing calcination temperature. Therefore, it is found that increasing calcination temperature increase the crystallinity of $Li_{1+x}Mn_{2-\delta}O_4$ powders, but reduces the average oxidation state of manganese.

The final morphology of the calcined powder as a function of calcination temperature is given in Fig. 6. It is clear that the mean particle size increases with increasing calcination temperature. The shape is changed to facet shape with high calination temperature.

3.2. Electrochemical characterization

Charge/discharge curves for $LiMnO_4$ samples, calcined at different temperatures, in Li/1 M $LiClO_4$-PC solution/$LiMn_2O_4$ cells are shown in Fig. 7. The sample calcined at 600°C for 4 h yielded the lowest specific capacity (110 mAh/g) for discharge. The sample calcined from 700 to 850°C for 4 h yielded similar specific capacity for both charge and discharge. We can predict that the sample calcined at high temperature will increase specific capacity for charge due to low oxidation state of manganese. But cell polarization increased due to decreased surface area for larger particles at high calcinations temperature. So, the calcined powder 800°C, 850°C didn't charge fully to 4.3 V. If the cut-off voltages were set higher to 4.5 V, the temperature dependence of specific capacity for charge will be increase due to lowering Mn valence state at high temperature heat treatment [13, 14].

The cycling performance for each condition of powder preparation is shown in Fig. 8. The cycle life of the cathode is improved by decreasing the calcination

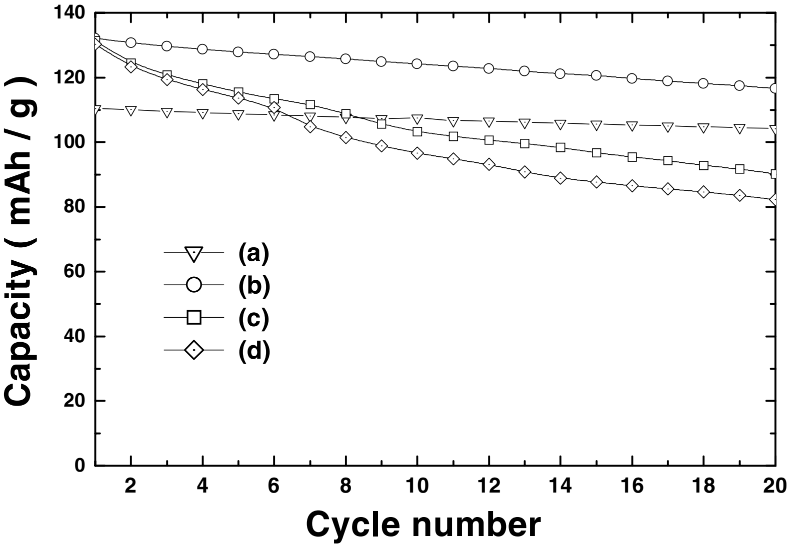

Figure 8 Discharge capacity of Li/$LiMn_2O_4$ cell according to calcination temperature: (a) 600°C for 4 h, (b) 700°C for 4 h, (c) 800°C for 4 h and (d) 850°C for 4 h (0.2C).

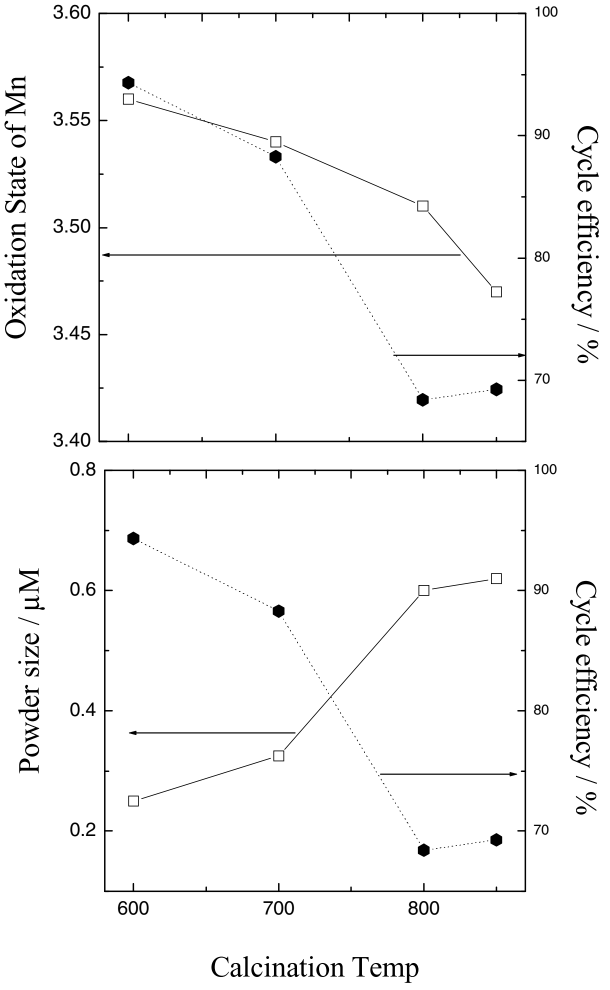

Figure 9 Capacity retention of Li/$LiMn_2O_4$ cell according to calcination temperature as a function of powder size and Mn valence state.

temperature. This result is the same with that of Liu *et al.* [13]. We carefully investigated capacity fading mechanism as a function of powder size and Mn valence state in Fig. 9. The cathode calcined at low temperature (600°C) show high cycle efficiency near 94% (definition of capacity retention in this work = 20th discharge capacity/1st discharge capacity). The capacity retention sharply decreases with increasing calcination temperature. This decay tendency is compatible to lowering of Mn valence state and growing of particle size. The results indicate that Mn valence-state and powder size of cathode powder can be important variables to capacity fading of $LiMn_2O_4$ spinel.

4. Conclusions

In this work, $LiMn_2O_4$ spinel with a nominal composition was prepared by Pechini method as a function of calcination temperature, and cathodic properties and failure modes have been examined. The following observations are made.

(i) The samples calcined at low temperature have a smaller lattice constant than the ones calcined at high temperature. The morphology is changed from round to facet shape with higher temperature.

(ii) The sample calcined at 600°C for 4 h yielded the lowest specific capacity (110 mAh/g) for both charge and discharge. The sample calcined from 700 to 850°C for 4 h yielded similar high specific capacity (130 mAh/g) for both charge and discharge.

(iii) The capacity retention sharply decreases with increasing calcination temperature. This decay tendency is compatible to lowering of Mn valence state and growing of particle size. There appears to be a close relationship between Mn valence-state, powder size of cathode powder and their cathode capacity retention.

References

1. J. M. TARASCON, E. WANG, F. K. SHOKOOHI, W. R. McKINNON and S. COLSON, *J. Electrochem. Soc.* **138** (1991) 2859.
2. R. J. GUMMOW, A. DE. KOCK and M. THAKERAY, *Solid State Ionics* **69** (1994) 59.
3. D. H. JANG and S. M. OH, *J. Electrochem. Soc.* **144** (1997) 3342.
4. Y. XIA and M. YOSHIO, *ibid.* **143** (1996) 825.
5. D. AURBACH, I. WEISSMAN, A. ZABAN, E. MENGERITSKI and P. DAN, *ibid.* **143** (1996) 2100.
6. M. M. THACKERAY, A. DE KOCK and W. I. F. DAVID, *Mater. Res. Bull.* **28** (1993) 1041.
7. D. GUYOMARD and J. M. TARASCON, *Solid State Ionics* **69** (1994) 222.
8. J. M. TARASCON, W. R. McKINNON, F. COOWAR, T. N. BROWNER, G. AMATUCCI and D. GUYOMARD, *J. Electrochem. Soc.* **141** (1996) 1783.
9. M. P. PECHINI and A. ADAMS, US Patent. no. 3,330,697 (1963).
10. S. P. LIU, K. Z. FUNG, Y. M. HON and M. H. HON, *J. Cryst. Growth* **226** (2001) 148.
11. Y. S. HAN and H. G. KIM, *J. Power Sources* **88** (2000) 161.
12. Y. XIA and M. YOSHIO, *J. Electrochem. Soc.* **144** (1997) 4186.
13. W. LIU, G. C. FARRINGTON, F. CHAPUT and B. CUNN, *ibid.* **143** (1996) 879.
14. D. H. JANG and S. M. OH, *J. Korea Chem. Soc.* **42** (1998) 122.
15. M. M. THACKERAY, *J. Electrochem. Soc.* **142** (1995) 2558.
16. C. MASZUELIER, M. TABUCHI, K. ADO, R. KANNO, Y. KOBAYASHI, Y. MAKI, O. NAKAMURA and J. B. GOODENOUGH, *J. Solid State Chem.* **123** (1996) 255.

Received 7 July
and accepted 30 December 2003